Journal of Electronic Materials

MECHANISMS OF TWO-STAGE CONDUCTIVITY RELAXATION IN CdTe:Cl WITH ULTRASOUND

--Manuscript Draft--

Manuscript Number:	JEMS-D-19-01881
Full Title:	MECHANISMS OF TWO-STAGE CONDUCTIVITY RELAXATION IN CdTe:Cl WITH ULTRASOUND
Article Type:	S.I. : 2019 IC II-VI Compounds
Keywords:	ultrasound; CdTe single crystals; point defects; dislocation clusters; Hall effect; scattering mechanisms
Corresponding Author:	Mykola Tymochko, Ph.D. V.Ye. Lashkaryov Institut of Semiconductor Physics NAS of Ukraine Kyiv, UKRAINE
Corresponding Author Secondary Information:	
Corresponding Author's Institution:	V.Ye. Lashkaryov Institut of Semiconductor Physics NAS of Ukraine
Corresponding Author's Secondary Institution:	
First Author:	Yaroslav Olikh
First Author Secondary Information:	
Order of Authors:	Yaroslav Olikh
	Mykola Tymochko, Ph.D.
	Oleg Olikh
Order of Authors Secondary Information:	
Funding Information:	
Abstract:	We have investigated the kinetics of acoustic relaxation in low-ohmic n-CdTe:Cl crystals in the temperature range 77÷200 K when ultrasound (longitudinal waves with a frequency ~ 10 MHz and an intensity ~ 104 W/m2) was switched on/off. We found out acoustic conductivity relaxation to occur in two stages. Fast (<0.6 s) relaxation stage is mainly related to the charge carrier concentration changes and, in part, can be determined by acoustically induced changes of the scattering at dislocations and neutral impurities; the long (>40 s) stage is mainly caused by the charge carriers mobility changes due to scattering at ionized impurities. We also have discussed possible acoustically stimulated restructuring of point-defective complexes in adjacent crystal regions.
Suggested Reviewers:	Arturs Medvids, PhD, Doc.habil.Ph. Professor (Full), Institut of Technical Physics, Riga Technical University medvids@latnet.lv https://www.researchgate.net/profile/Arturs_Medvids2 https://scholar.google.com/citations?user=GvU1Z0EAAAAJ&hl=uk&oi=ao DOI: 10.1002/pssc.201600052
	Petro Fochuk Professor, vice-rector, Chernivtsi National University fochukp@gmail.com https://www.researchgate.net/profile/Petro_Fochuk2 https://scholar.google.com.ua/citations?user=gRaqOOAAAAAJ&hl=uk DOI: 10.1109/TNS.2016.2583546
	Ion Ion Geru Institute of Chemistry of Academy of Sciences of Moldova iongeru11@gmail.com

	https://www.researchgate.net/profile/Ion_Geru
	Dmytro Vasyl'ovych Korbutyak Institute of Semiconductor Physics NAS of Ukraine kdv45@isp.kiev.ua https://link.springer.com/article/10.1134/S1063782615070209

MECHANISMS OF TWO-STAGE CONDUCTIVITY RELAXATION IN CdTe:Cl WITH ULTRASOUND

Ya. Olikh[1,3], M. Tymochko[1,4], O. Olikh[2]

[1]*V.E. Lashkaryov Institute of Semiconductor Physics*, NAS of Ukraine, 41, pr. Nauky, Kyiv 03028, Ukraine.

[2]*Physics Faculty, Taras Shevchenko National University of Kyiv, Kyiv, 01601, Ukraine.*

3.–e-mail: jaroluk3@ukr.net.

4.–e-mail: tymochko@ukr.net.

ABSTRACT

*We have investigated the kinetics of acoustic relaxation in low-ohmic n-*CdTe:Cl *crystals in the temperature range* 77÷200 K *when ultrasound (longitudinal waves with a frequency* ~ 10 MHz *and an intensity* ~ 10^4 W/m^2) *was switched on/off. We found out acoustic conductivity relaxation to occur in two stages. Fast* (<0.6 s) *relaxation stage is mainly related to the charge carrier concentration changes and, in part, can be determined by acoustically induced changes of the scattering at dislocations and neutral impurities; the long* (>40 s) *stage is mainly caused by the charge carriers mobility changes due to scattering at ionized impurities. We also have discussed possible acoustically stimulated restructuring of point-defective complexes in adjacent crystal regions.*

Key words: ultrasound, CdTe single crystals, point defects, dislocation clusters, Hall effect, scattering mechanisms.

INTRODUCTION

The physical properties of real crystals containing structural defects depend not only on the defects concentration, but also essentially feel the nature of their interaction. In particular, in binary crystals of A_2B_6 and A_3B_5 solid solutions characterized by high dislocation density (N_{dis}~ 10^{10} m^{-2}), the linear defect interaction with alloying impurities and their complexes can crucially influence on the conductivity. The role of dislocations also increases for films and nanostructures. Of course, uncontrolled electrically active defects deteriorate properties of semiconductor materials; however, it opens possibilities to change the structure of crystal defects by various external fields and to control physical characteristics of the material. Such data not only shows the prospect to control the properties of solids when processing them, but also allow us to expect possible changes in their properties during operation. For example, ultrasonic (US) loading of semiconductor crystals or devices can change the defects concentration, their state, and the nature of interdefect interaction so causing a change in the physical properties of the crystals and the working characteristics of devices [1-3].

One use CdTe crystals to detect radiation and construct solar cells [4-5]. However, defects (dislocations, blocks, inclusions, point defect complexes) limit their use. One of the ways to study the interaction of dislocations with other defects is acoustic-Hall method [1,6,7]. As dislocations are the main link to transmit ultrasound energy to electrically active point defects, the acoustical dislocation mechanism is determinative one. Depending on the sample impurity-defective structure and the ultrasound wave parameters, one can realize both residual and reversible changes observed only under ultrasound action. Dynamic studies give the most information on the mechanisms of the phenomenon; the reason of this, in particular, is high lability of the impurity-defective structure of A_2B_6 crystals under ultrasonic loading at low temperatures (<200 K) [2,8].

In earlier works [8,9], we investigated the ultrasound influence on the electrophysical characteristics of bulk single crystalline CdZnTe samples and studied the relaxation characteristics of the electrical conductivity $\sigma(t)$ under switching on/off the ultrasonic load. We found acoustically induced (AI) changes in $\sigma(t)$ to be reversible and after the ultrasonic loading finishes, a slow (40÷400) s restoration of the sample parameters occurs. Note that the nature of the AI relaxation of $\sigma(t)$ for different in dopant chlorine concentration CdTe samples may generally differ.

The paper presents the results of detailed complex electrophysical studies for CdTe:Cl crystal with a pronounced positive effect of AI changes in electrophysical characteristics at low temperatures [8]. We found that AI relaxation of $\sigma(t)$ occurs in at least two stages showing the presence of two ultrasound driven processes. To find out the mechanisms of them, we compared in detail temperature characteristics of short-term (ST) and long-term (LT) electroconductivity changes in CdTe:Cl samples under switching on/off US with corresponding changes in the relative contribution of the electron concentration and mobility into the conductivity.

SAMPLES AND METHODS

The CdTe:Cl single crystals were grown by the Bridgman vertical method at low Cadmium vapor pressure in the ampoule and chlorine doped ($N_{Cl} \approx 10^{24}$ m^{-3}) [10]. The X-ray topography method (Williamson-Hall construction) estimated the helical dislocations density $N_{dis}^{XR} \approx 4 \cdot 10^9$ m^{-2} [9]. We form the ohmic contacts for the samples by the method of thermal vacuum pollination of indium at 164°C. We measured concentration $n(T)$ and the mobility $\mu_H(T)$ of current carriers in the temperature range (77÷200) K by the Hall method in the mode of constant electric and magnetic fields. The magnetic field and propagation of the longitudinal ultrasonic wave were parallel to the direction [110] (see the inset in Fig. 1). The selected non-piezoactive direction of the acoustic wave propagation eliminates the action of the local piezo field [11]. Note also that the US amplitude ($W_{US} \approx 10^4$ W/m^2) used here did not cause deformations exceeding the dynamic material yield point; therefore, AI dislocation propagation did not occur, as completely reversible nature of ultrasound loading influence on the electrophysical (EP) characteristics of the samples shows.

When investigating the EP parameters under ultrasound loading, we used a nitrogen cryostat equipped with acoustic elements. We described the measurement technique in detail in [1,6-9]. We investigated $\sigma(t)$ relaxation dependences in the same cryostat under switching on/off the load using a digital multimeter and a related PC. We have performed dynamic study of $\sigma(t)$ by steps of ~0.6 s. The temperature fluctuations δT due to ultrasonic heating ranged from 0.1 to 4 K were took into account in the quantitative calculations of $\sigma(t)$.

RESULTS

Ultrasound influence on electrophysical characteristics

Figure 1a shows electrical conductivity $\sigma(T)$ temperature dependences for both the original sample and ultrasonically loaded. For low temperatures (T<200 K), we observed AI changes in $\sigma_i(T)$ dependence. To make clear the mechanisms of change in $\sigma_i(T)$ under ultrasound loading, it is important to separate AI changes in carrier concentration and mobility. It was done by measuring the Hall effect. We calculated $n_e = (eR_H)^{-1}$ and $\mu_H = R_H\sigma$ in the standard way; Figs. 1b and 1c show their temperature dependences. Under ultrasonic loading (curve 2) the electron concentration increases. At room temperature it is non-essential, however, at nitrogen temperatures AI changes reach about 20%. Note that $n(T)$ is monotonous in the whole temperature range, both in the original sample and ultrasonically loaded, being in general slightly dependent on temperature. Fig. 1c show temperature dependences of separate scattering components, which were obtained by nonlinear approximation of the experimental dependences $\mu_{exp}(T)$ [12]. More details see below.

Relaxation of conductivity when the ultrasound is switched on/off

AI $\sigma(t)$ changes are completely reversible and even long (hour and more) ultrasonic loading does not cause residual changes in the crystal parameters. We found out that AI relaxation comes about in two stages (Fig. 2a, b). When switching on/off, we see a short (for time <0.6 s) conductivity $\Delta\sigma_{US}^s$ ($\Delta\sigma_0^s$) change, after that there is a long-term monotonic relaxation $\Delta\sigma_{US}^l$ ($\Delta\sigma_0^l$). Therefore, the conductivity change has two components, ST and LT in the selected notations (see Fig.2a, b) $\sigma_{US} = \sigma_0 + \Delta\sigma_{US}^s + \Delta\sigma_{US}^l$ and $\sigma_0 = \sigma_{US} - \Delta\sigma_0^s - \Delta\sigma_0^l$. Moreover, $\Delta\sigma_0^s \neq \Delta\sigma_{US}^s$, $\Delta\sigma_0^l \neq \Delta\sigma_{US}^l$. Here, σ_0 and σ_{US} are the initial (before turning on the ultrasound) and stationary at ultrasonic loading $\sigma(t)$ values, resp. The first stage τ_s goes on <0.6 s; we haven't investigated the kinetics of this stage in more detail. The time of the second stage τ_l is (40 – 400) s and increases with decreasing in sample temperature.

Temperature dependences of ST and LT conductivity changes relaxation components

Figure 3 shows the temperature dependences of the increase / decrease in the absolute value of the short-term (($\Delta\sigma_{US}^s$ and $\Delta\sigma_0^s$) and the long-term (($\Delta\sigma_{US}^l$ and $\Delta\sigma_0^l$) components of AI sample conduction change. One can see at Fig. 3 that the rate

of temperature changes for the long-term components of the increase / decrease in conductivity is much higher (about 6 times) than for the ST ones. It confirms qualitative difference between ultrasound action at instantaneous and LT relaxation stages. In particular, the weak temperature dependence for $\Delta\sigma_{US}^{s}$ and $\Delta\sigma_{0}^{s}$ shows athermic nature of the process.

Figure 4 shows the ST and LT contributions in the total change of $\sigma(t)$. One can see that temperature dependencies of ST and LT fraction are opposite.

Temperature dependences of electron concentration and mobility contributions

As the concentration of carriers and their mobility control CdTe conductivity $\sigma(T)=e\cdot n(T)\cdot\mu(T)$, we can assume that ST and LT $\sigma(t)$ depend on the change of one of these parameters only. To verify the assumption, we take experimental data on $n_e(T)$ and $\mu_i(T)$ and calculated the temperature dependences of the relative changes in the carrier concentration and their mobility: $\delta n=(n_{US}-n_0)/n_0$, $\delta\mu=(\mu_{US}-\mu_0)/\mu_0$, $\delta\sigma=(\Delta\sigma_{US}-\sigma_0)/\sigma_0$. Then we calculated relative contributions of them to $\sigma(T)$ by the following relations: $\Delta_\sigma^n(T) = \delta n/\delta\sigma$ and $\Delta_\sigma^\mu(T) = \delta\mu/\delta\sigma$. These dependences of $\Delta_\sigma^n(T)$ and $\Delta_\sigma^\mu(T)$ are shown in Fig. 5. When the temperature decreases, $\Delta_\sigma^n(T)$ weakens, however, $\Delta_\sigma^\mu(T)$ increases.

DISCUSSION

Comparison of temperature characteristics of AI changes in conductivity relaxation time components with concentration and mobility contribution to the conductivity

Comparison of Fig. 4 and Fig. 5 shows the correlation of the temperature changes of ST and LT contributions with the temperature changes of the concentration and mobility contributions to the conductivity $\sigma(T)$, resp. Therefore, we can assume that the process prompting an ST relaxation of $\sigma(T)$ is predominantly determined by the acoustic concentration effects; at the same time AI long-term relaxation processes are mainly related to AI changes in mobility.

Comparison of the LT stage of the acoustic conductivity kinetics with photoconductivity

Figs. 2a and 2b illustrate similarity between acoustic conductivity (AC) LT phase and the kinetics of photoconductivity (PC) in high-resistance inhomogeneous CdTe semiconductor crystals [13-14]. We use this formal similarity to reconstruct the LT $\sigma(t)$ relaxation curves in Fig. 2a, b, according to the scheme used to analyze PC kinetics. We rebuild them in the following scale: when turned on $(-\ln(1-(\sigma-\sigma_0)/(\sigma_{US}-\sigma_0)) = t/t_{on}$, and when switched off $\ln(\sigma-\sigma_0) = (-t/t_{off})$ (see Fig. 2 c, d). Here, t_{on} and t_{off} are relaxation time constants of LT stage when the ultrasound is switched on/off, resp. First, we analyze the recovery curve (Fig.2d), where the process goes without ultrasound. We see that the $\sigma(t)$ decrease passes along an exponential with characteristic time $t_{off}\approx$32,4 s. As for the LT of the $\sigma(t)$ growth stage when the US is turned on (Fig. 2c), taking the general

temperature changes (Fig. 2a), we can assume that the process has also thermoactivating part, and, similar to the PC growth stage, it is not unique; both the AI $\sigma(t)$ growth occurs and there is a partial recovery in accordance with the process $\ln(\sigma-\sigma_0)=(-t/t_{off})$ (see Fig. 2d). When saturation occurs, a dynamic equilibrium becomes between the rate of return to initial state and the rate of AI perturbation ($\sigma(t)$ growth). The average time constant in this case is $t_{on} \approx 12{,}4$ s.

However, despite the formal similarity of AC with PC, we emphasize the fundamental difference between them. In PC case, changes in $\sigma(t)$ are only related to carrier concentration; in the case of AC, there are both changes of concentration and mobility. In PC, quantum processes with electron redistribution between the levels (traps) and the conduction band are primary when the light is turned on, and only then certain diffusion long-term restructuring processes can occur in the point defect (PD) system caused by the change of the intra-crystalline electric field [3,11]. In the case of AI processes, at the moment of ultrasound switching on, first the restructuring of PD complexes near oscillating dislocation segments happens. These may be, in particular, metastable centers changing the charge (Jan-Teller effect) [15,16] due to their lattice position (orientation) change. In the process of AI dislocations oscillations, a new topography of local mechanical and electrical fields occurs causing restructuring not only in the PD clusters, but also in dislocations structure [17,18]. The difference between the AC and the PC also reflects in the distinct duration of the characteristic $\sigma(t)$ relaxation at growth and recovery, resp. Indeed, when the ultrasound is switched on, the relaxation time is almost 2 times shorter than when it is switched off (Fig. 2). This experimental fact also confirms the diffusive nature of the AI local rearrangement of the point-defective crystal structure; as we know, diffusion coefficient increases under US loading [19, 20]. At the same time, the complete recovery of the relaxation curves at repeated ultrasound switching on at a fixed temperature shows the stability of the dislocation structure.

Temperature characteristics for separate contribution of individual carrier scattering components

It is known that mobility value is determined by different mechanisms of charge carrier scattering. The temperature dependences of the contribution of separate scattering mechanism were estimated as following. The scattering on neutral impurities, ionized impurities and dislocations were under consideration. According to the Mattisen rule [21,22]:

$$1/\mu_{exp}^{0,US} = \Sigma(1/\mu_i^{0,US}) = 1/\mu_N^{0,US} + 1/\mu_{dis}^{0,US} + 1/\mu_{ii}^{0,US}, \quad (1)$$

were μ_{exp} is the experimental value, $\mu_i^{0,US}$ are the calculated mobility components when scattering on neutral impurities ($\mu_N^{0,US}$), dislocation scattering ($\mu_{dis}^{0,US}$), scattering on ionized impurities ($\mu_{ii}^{0,US}$), resp; superscript “0” and “US” correspond to sample without ultrasound and with it, resp. The scattering by the lattice phonons is negligible for low temperatures where AI $\sigma(t)$ relaxation is observed.

The experimental temperature dependences of $\mu_{exp}(T)$ were fitted by Eq. (1) with help of method of differential evolution [12] and contributions of different mechanism were estimated - see Fig. 1c. The more details about fitting procedure are given elsewhere [9], but main AI effects were the following.

i) the scattering on neutral impurities increases; the reason for the increase in neutral impurities concentration (from $4.6 \cdot 10^{23}$ m^{-3} to $15.3 \cdot 10^{23}$ m^{-3}) is recharge (ionization) of certain centers and decay of complexes;

ii) the dislocation scattering, in our opinion thus deals with a decrease in concentration of charged centers, located in the adjacent regions of the crystal;

iii) the scattering on the ionized impurities weakens by reducing their effective concentration (from $5.5 \cdot 10^{23}$ m^{-3} to $2.2 \cdot 10^{23}$ m^{-3}).

Figure 6 shows the temperature dependences of AI relative changes in the mobility components:

$$\Delta_i(T)=(\Delta^{US}(\mu_i)) / (\Delta^{US}(\mu_{exp})) \qquad (2),$$

where

$$\Delta^{US}(\mu_{exp}) = 1 / [(1/\mu_{exp}{}^{US}) - (1/\mu_{exp}{}^{0})]; \ \Delta^{US}(\mu_i) = 1 / [(1/\mu_i{}^{US}) - (1/\mu_i{}^{0})] \qquad (3).$$

In Fig. 6, all three components change with temperature decrease; however, the rates are different: $(\partial(\Delta_{ii}{}^{US}(\mu_{ii})/\partial T) = 0{,}31$ K^{-1}); $(\partial(\Delta_{dis}{}^{US}(\mu_{dis})/\partial T) = 0{,}08$ K^{-1}, and $(\partial(\Delta_N{}^{US}(\mu_N)/\partial T) = -0{,}12$ K^{-1}. The highest temperature growth rate of the mobility component happens on ionized impurities being (3-÷4) times higher than the rate of change of the dislocation scattering parts and that on the neutral impurities. The time ranges of scattering mechanisms in $\sigma(t)$ relaxation is separated by comparing the value of $\partial(\Delta_i(T))/\partial T$ (Fig. 6) with the coefficients of temperature changes of the ST and LT components (Fig. 3). Dislocation and neutral impurities scattering parts characterized by small temperature change rates close to the ST part, we refer to the factors determining the ST of $\sigma(t)$. In our opinion the dislocation scattering part can compensate negative character of ultrasound influence on neutral impurities component, especially because their temperature change rates are close. The scattering on ionized impurities $\Delta_{ii}(T)$ changes most with temperature and is responsible for the AI growth of $\sigma(t)$, and is attributed to the LT stage reason.

Features of inhomogeneities influence on AI conductivity changes

Consider another important factor influencing CdTe conductivity. The low values of mobility in samples at room temperatures show a significant contribution to the scattering of charge carriers on crystal heterogeneity due to the accumulation of impurities in CdTe:Cl [23,24]. How can this mechanism show itself under ultrasound? We already suggested [8] that intensive US loading essentially weakens the inhomogeneities influence. The mechanism of such σ growth is AI fluctuation decrease of the crystal potential relief. The $\Delta_N(T)$ dependence (Fig. 6) formally characterizes not only AI change of

neutral impurities concentration N_N, but also the total electron scattering on the neutral impurity complexes contribution change.

As for the kinetics of AI changes, it is worth to emphasize that such AI processes are athermic (the rate of state change coincides with the rate of external deformation change), ie changes in the inhomogeneities characteristics usually happen through several periods of US loading. Therefore, we see the influence mainly in ST stage. In fact, the weak temperature dependence of $\Delta_N(T)$ (Fig. 6) directly confirms these assumption.

Acoustical dislocation mechanism of crystal defect structure rebuilding

As we already noted, the dislocations motion causes not only changes in the charge carriers scattering. Their main manifestation in AI processes in A_2B_6 crystals is, in fact, mechanical stresses of the acoustic wave localized in the scale of the crystal lattice and point defects determining the physical properties of a semiconductor crystal. One can see in Fig. 6 that the largest contribution of AI changes in the CdTe:Cl crystal is the scattering decrease on ionized impurities (μ_{ii}). Previous calculations make it clear that this thermoactivating mechanism causes the LT $\sigma(t)$ change.

Let us dwell in more detail at the AI LT structural rearrangements near dislocation clusters that, in general, determine the temporal nature of the LT. When the US is switched on for (10^{-6}–10^{-5}) s, the sample volume oscillates with the US wave frequency; including PD clusters centered mainly around dislocations. As a result of the forced dislocations oscillations (with an amplitude up to $\leq 10^{-8}$m), the area of effective interaction of dislocations with electrons at traps enlarges; also electrons release from impurity levels [8,9,17]. One can assume that concentration increase Δn with the atom oscillation amplitude in the US relates to an increase of the capture radius during the US process, ie an increase of the area sweeping by dislocations [9,17]. In the course of the US, the distribution of dislocations segments involved in AI oscillations can vary in length by thermo-activation (ie long-term), and there is a partial separation from weakly coupled centers of attachment. However, over time, the conditions of dislocations motion somewhat change. Even some reorganization of the dislocation structure is possible [25].

This process can cause capturing many point defects (including charged ones, that reduces the ionized centers concentration N_{ii}) by dislocation traps and, then, to the expansion of the region enriched by them [26]. As a result, potential barrier reduces; a non-stationary state of the PD structure occurs that seeks to adjust according to the new quasi-stationary electric-deformation conditions. These restructurings involve also some local acoustochemical reactions [27].

We explain the increase of AI effects with temperature decrease by a corresponding decrease of phonon friction, whose magnitude mainly determines dislocations motion in semiconductor crystals, ie, an increase of the velocity (and amplitude) of dislocations oscillation [11, 26].

CONCLUSIONS

To find out the mechanisms of relaxation of the acoustic conductivity $\sigma_{US}(t)$ in low-resistance *n*-CdTe crystals ($N_{Cl} \approx 10^{24}$ m^{-3}) in the temperature range (77 -÷ 300) K, we investigated its kinetics at ultrasound switched on/off.

Separate comparison of the temperature dependences of the amplitudes of $\sigma_{US}(t)$ individual stages with the corresponding temperature changes in concentration and mobility allows to associate acoustically induced concentration effects mainly with short-term (<0.6 s) $\sigma_{US}(t)$ changes and AI effects of mobility changes mostly with long-term (>40 s) ones.

Further analysis of the temperature characteristics for the separate mobility components contribution determined by certain mechanisms of carrier scattering make it possible to clarify their contribution to the ST or LT relaxation phase of $\sigma_{US}(t)$. Namely, we attribute the scattering mechanisms controlling the dislocation and neutral impurity components of mobility to the factors that mainly (along with concentration ones) control the short-term changes, while the scattering on ionized impurities – to long-term ones.

It is suggested that possible mechanisms of acoustically induced conductivity changes are the transformation of the point-defect complexes mainly in the near dislocation crystal regions and fluctuation decrease of the crystal potential relief consequently.

ACKNOWLEDGMENT

We express our gratitude to the employees of the Chernivtsi National University M.I. Ilashchuk, A.A. Parfenyuk, and K.S. Ulyanytskyi for supplying us with CdTe samples to investigate, and to Dr. W.H. Kozyrski at Bogolubov Institute for Theoretical Physics for useful discussion.

REFERENCES

1. A.I. Vlasenko, Ya.M. Olikh, and R.K. Savkina, *Semiconductors* 33, 398 (1999). https://doi.org/10.1134/1.1187701.
2. V. Babentsov, S.I. Gorban, I.Ya. Gorodetskiy, N.E. Korsunskaya, I.M. Rarenko, and M.K. Sheinkman, *Sov. Phys. Semicond*. 25, 1243 (1991).
3. O.Ya. Olikh, *Superlattices Microstruct*. 117, 173 (2018). https://doi.org/10.1016/j.spmi.2018.03.027.
4. D.V. Korbutyak, S.W. Mel'nychuk, E.V. Korbut, and M.M. Borysyk, *Cadmium Telluride: Impurity-Defect States and Detector Properties* (Kyiv: Ivan Fedorov, 2000) (in Ukrainian).
5. I. Turkevych, R. Grill, J. Franc, E. Belas, P. Hoschl, and P. Moravec, *Semicond. Sci. Technol*. 17, 1064 (2002). doi:10.1088/0268-1242/17/10/305.
6. A.I. Vlasenko, Ya.M. Olikh, and R.K. Savkina, *Semiconductors*. 33, 398 (1999). doi:10.1134/1.1187701.
7. Ya.M. Olikh and M.D. Tymochko, *Tech. Phys. Lett*. 37, 37 (2011). https://doi.org/10.1134/S106378501101007X.

8. Ya.M. Olikh and M.D. Tymochko, Superlattices Microstruct. 95, 78 (2016). https://doi.org/10.1016/j.spmi.2016.04.038.

9. Ya.M. Olikh, M.D. Tymochko, O.Ya. Olikh, and V.A. Shenderovsky. *J. Electron. Mater*. 47, 4370 (2018). https://doi.org/10.1007/s11664-018-6332-4.

10. M.I. Ilashchuk, A.A. Parfenyuk, and K.S. Ulyanitskyi, *Ukr. J. Fiz*. 31, 126 (1986).

11. I.P. Golyamina, eds., *Ultrasound. The Small Encyclopedia* (Moscow: Soviet Encyclopedia, 1979) (in Russian).

12. O.Ya. Olikh, *J. Appl. Phys*. 118, 024502 (2015).

13. M.K. Sheinkman and A.Ya. Shik, *Sov. Phys. Semicond*.10, 209 (1976).

14. A.A. Ronassi and A.K. Fedotov. *Vestnik BGU*, Seriya 1. No.2. 8 (2010).

15. B. N. Mukashev, Kh. A. Abdullin, and Yu. V. Gorelkinskii, *Phys. Usp*. 43, 139 (2000).

16. N. S. Averkiev, I. B. Bersuker, V. V. Gudkov, K. A. Baryshnikov, I. V. Zhevstovskikh, V. Yu. Mayakin, A. M. Monakhov, M. N. Sarychev, V. E. Sedov, and V. T. Surikov. *J. Appl. Phys.* 116, 103708 (2014); https://doi.org/10.1063/1.4895475

17. Yu.A. Osipyan, eds., *Electronic Properties of Dislocations in Semiconductors* (Moscow: Editorial URSS, 2000) (in Russian).

18. N.A. Tyapunina, G.V. Bushueva, G.M. Zinenkova, E.K. Naimi, S.S. Novikov, *Crystallogr. Rep*. 55. 77 (2010). https://doi.org/10.1134/S106377451001013X.

19. V.N. Pavlovich, *Phys. Status Solidi B*. 180, 97 (1993).

20. O.Ya. Olikh and I.V. Ostrovsky, *Fiz. Tverd. Tela*. 44. 1198 (2002).

21. V.L. Bonch-Bruevich and S.G. Kalashnikov, *Semiconductor Physics* (Moscow: Nauka, 1977) (in Russian).

22. E.V. Kuchis, *Galvanomagnetic Effects and Investigation Methods* (Moscow: Radio i svjaz', 1990) (in Russian).

23. M.V. Alekseenko, E.N. Arkadyeva, and A.A. Matveev, *Sov. Phys. Semicond*. 4, 349 (1970).

24. B.I. Shklovskii and A.L. Efros, *Electronic Properties of Doped Semiconductors* (Berlin: Springer, 1984).

25. G.V. Bushueva, G.M. Zinenkova, N.A. Tyapunina, V.T. Degtyarev, A.Yu. Losev, F.A. Plotnikov, *Crystallogr. Rep*. 53. 474 (2008). https://doi.org/10.1134/S1063774508030152.

26. T. Suzuki, S.Takeuchi, H. Yoshinaga. *Dislocation Dynamics and Plasticity* (Moscow: Mir, 1989) (in Russian).

27. V.L. Gromashevskyi, V.V. Dyakin, E.A. Sal'kov, S.M. Sklyarov, N.S. Khilimova. *Ukr. J. Fiz*. 29, 550 (1984).

Fig. 1. CdTe: Cl. Temperature dependences of conductivity (a), electron concentration (b), and Hall mobility (c) with calculated mobility components for scattering at dislocations μ_{dis}, neutral impurities μ_N and ionized ones μ_{ii}; under ultrasound "US" and without it "0". In all the figures, curves 1 correspond to the initial samples, curves 2 to ultrasonic loading $W_{US}\approx10^4$ W/m^2, and curves 3 to the temperature dependences of the acoustically induced change. The inset in Fig. 1a shows the scheme of the acoustic cell: a is the sample, b is the buffer, c is piezoelectric transducer, HF is high frequency, US is longitudinal ultrasonic wave.

Fig. 2. CdTe:Cl. Typical oscillograms for $\sigma(T)$ at $T\approx121$ K, where the selected benchmark time milestones are marked for σ_i: a) when the ultrasonic load is switched on $\sigma_{US}= \sigma_0 + \Delta\sigma_{US}^s +\Delta\sigma_{US}^l$; b) when US is switched off $\sigma_0 = \sigma_{US} -\Delta\sigma_0^s -\Delta\sigma_0^l$; c) LT increase curve recovery from oscillogram US-on (a) in the scale $(- \ln(1-(\sigma-\sigma_0)/(\sigma_{US}-\sigma_0)) = (t/t_{on})$; d) decrease curve recovery from oscillogram US-off (b) in the scale $\ln(\sigma-\sigma_0)= (-t/t_{off})$. Solid lines in Fig (c) and (d) are linear approximations.

Fig. 3. CdTe:Cl. Experimental temperature dependences for absolute magnitude growth / decrease of ST ($\Delta\sigma_{US}^s$ and $\Delta\sigma_0^s$ – curves 1) and LT ($\Delta\sigma_{US}^l$ and $\Delta\sigma_0^l$ – curves 2) components of AI conductivity changes when ultrasound is switched on (a) and switched off (b).

Fig. 4. CdTe:Cl. Experimental temperature dependences for growth / decrease of AI components relative values for «instantaneous» ($\Delta\sigma_{US}^s / \Delta\sigma_{US}$ and $\Delta\sigma_0^s / \Delta\sigma_0$ – curves 1) and LT ($\Delta\sigma_{US}^l / \Delta\sigma_{US}$ and $\Delta\sigma_0^l / \Delta\sigma_0$ – curves 2) changes of sample conductivity when ultrasound is switched on (a) and switched off (b).

Fig. 5. CdTe:Cl. Temperature dependences of electron concentration $\delta n=(n_{US}-n_0)/n_0$ (curves 1) and mobility $\delta\mu=(\mu_{US}-\mu_0)/\mu_0$ (curves 2) relative parts in the total AI conductivity change $\delta\sigma=(\sigma_{US}-\sigma_0)/\sigma_0$, obtained in Hall measurements.

Fig. 6. CdTe:Cl. Temperature dependences of AI relative changes of mobility components for various scattering mechanisms, namely, on ionized impurities Δ_{ii}, on dislocations Δ_{dis}, and on neutral impurities Δ_N.

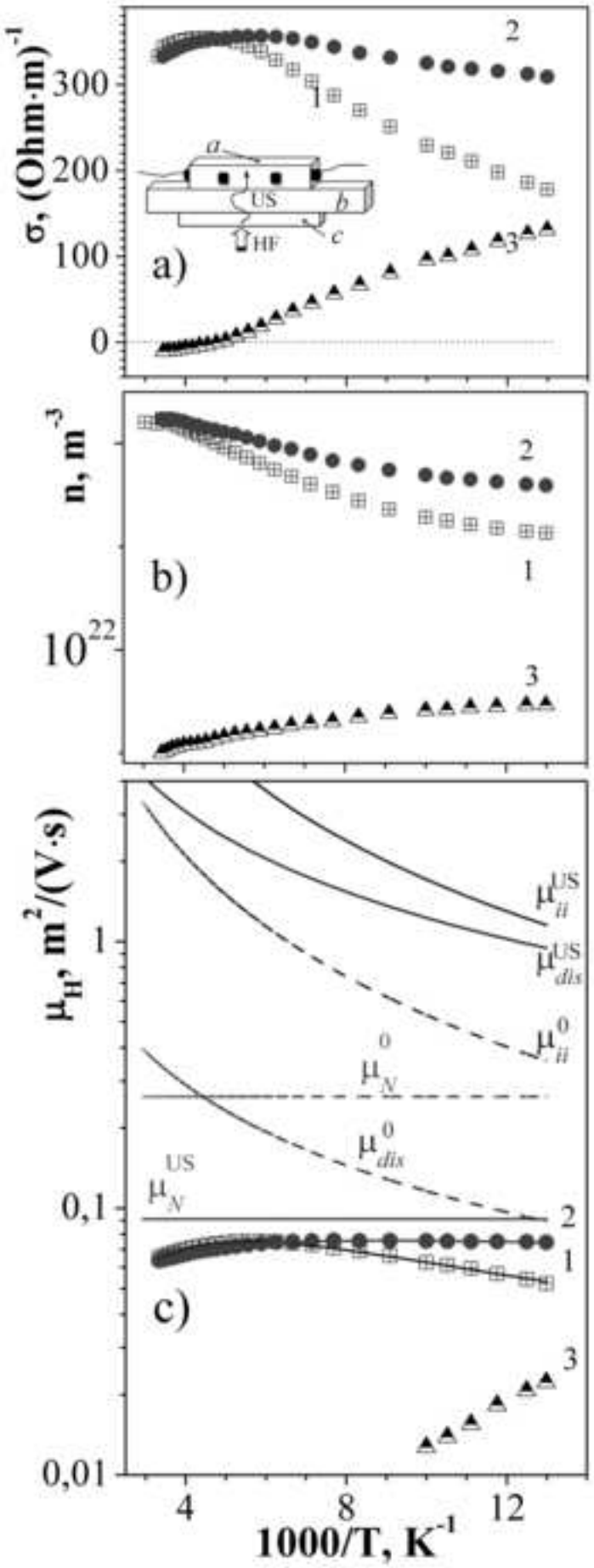

Figure

Click here to download Figure Fig. 2.jpg

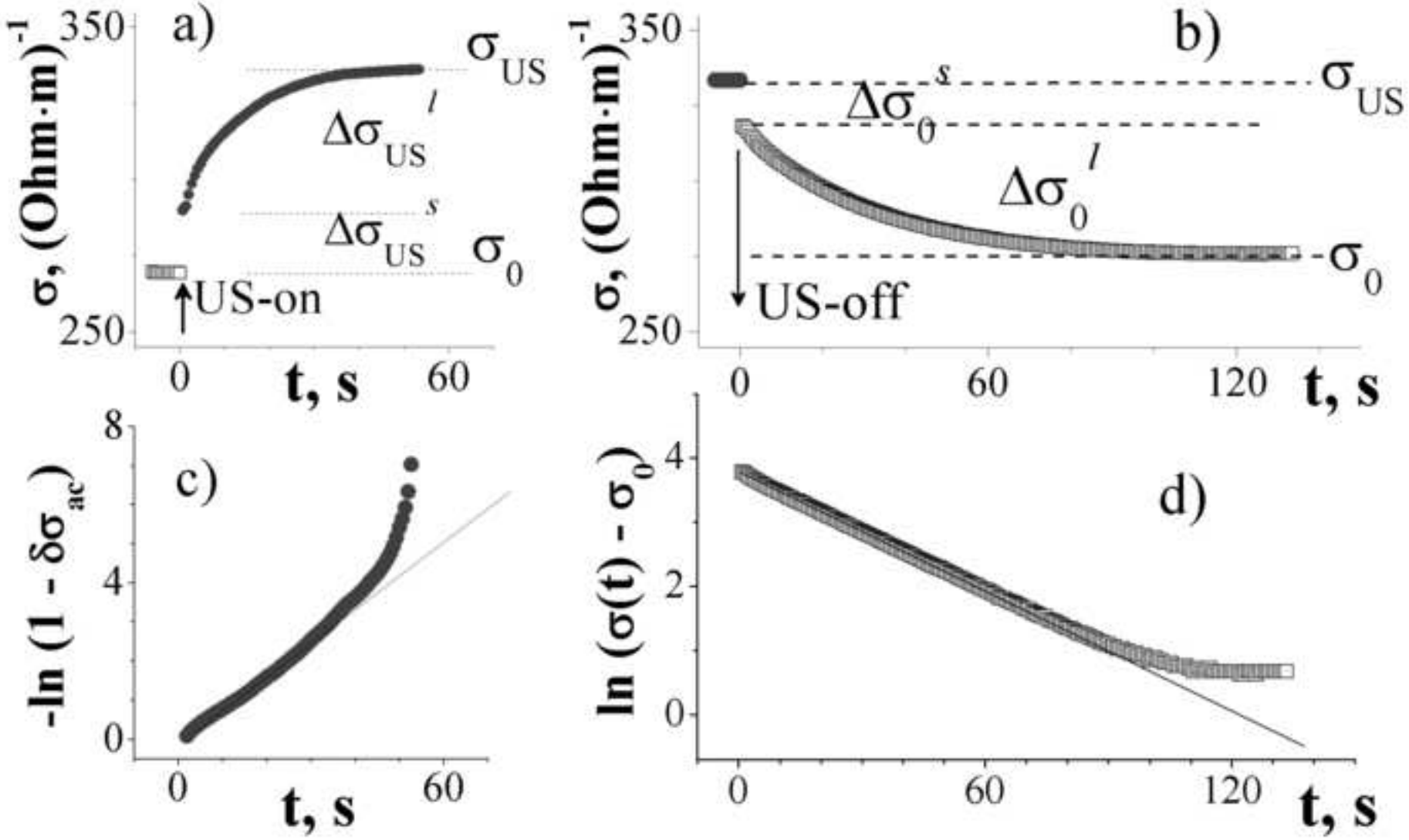

Figure

Click here to download Figure Fig. 3a.jpg

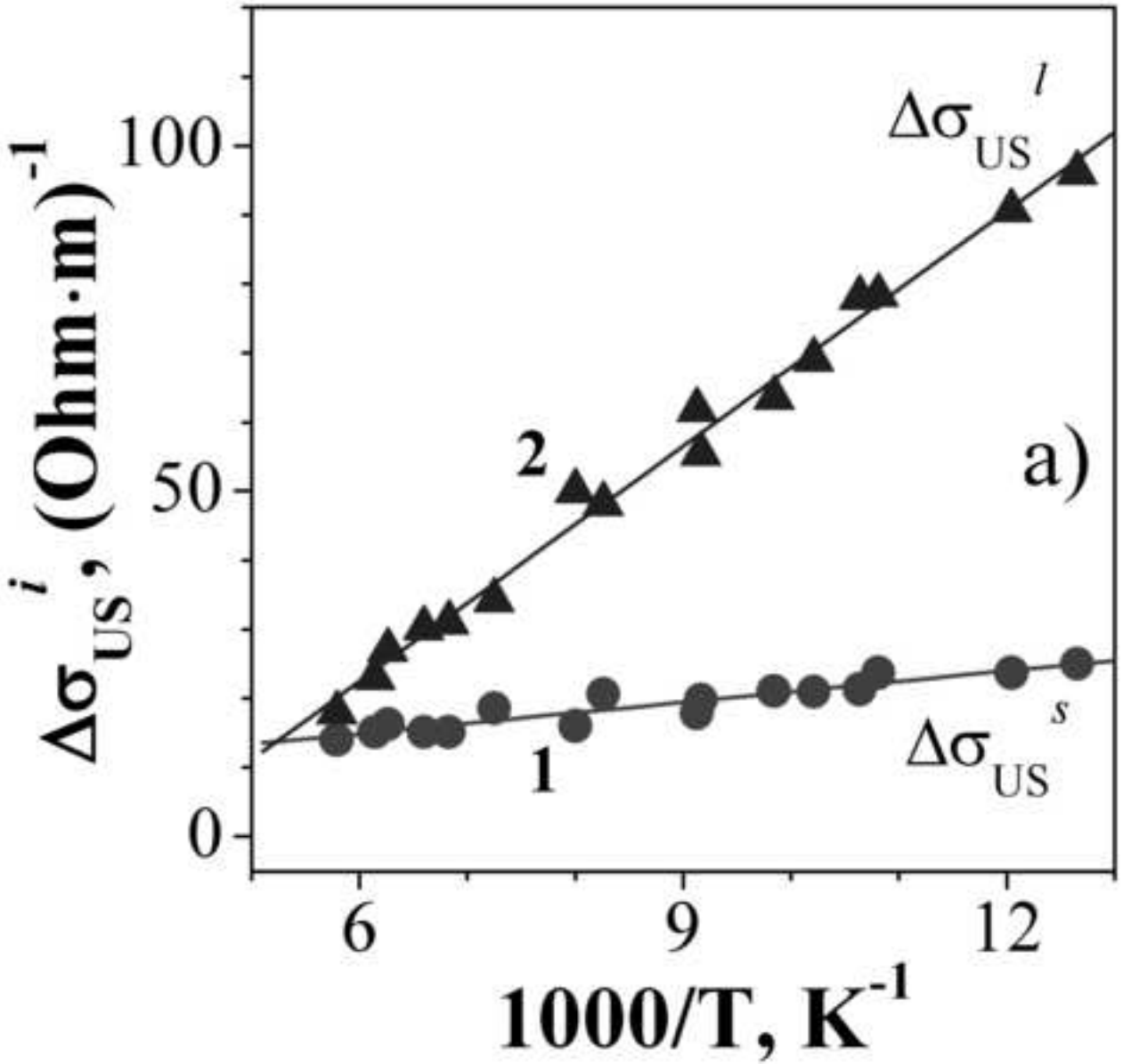

Figure

Click here to download Figure Fig. 3b.jpg

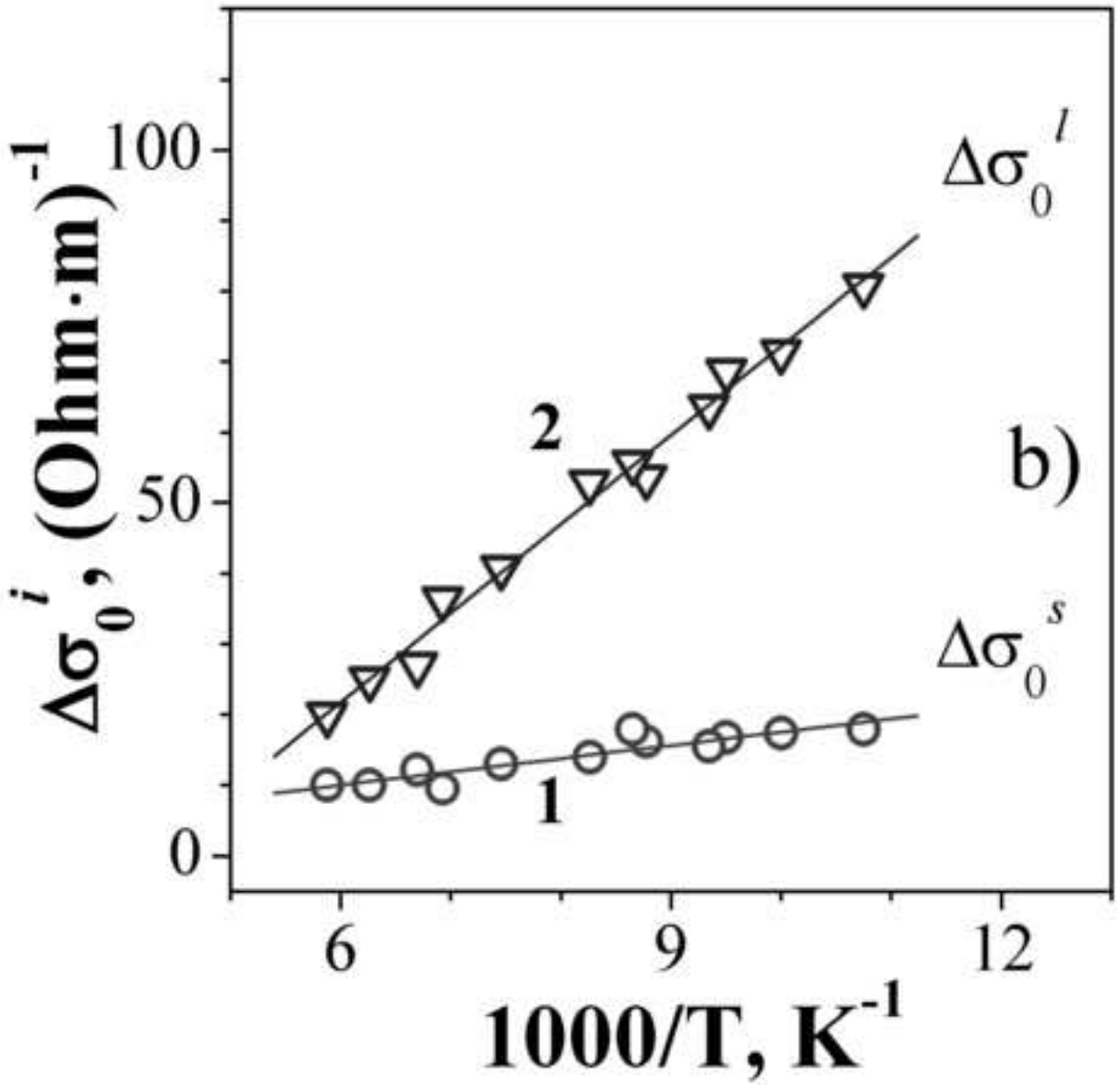

Figure

Click here to download Figure Fig. 4a.jpg

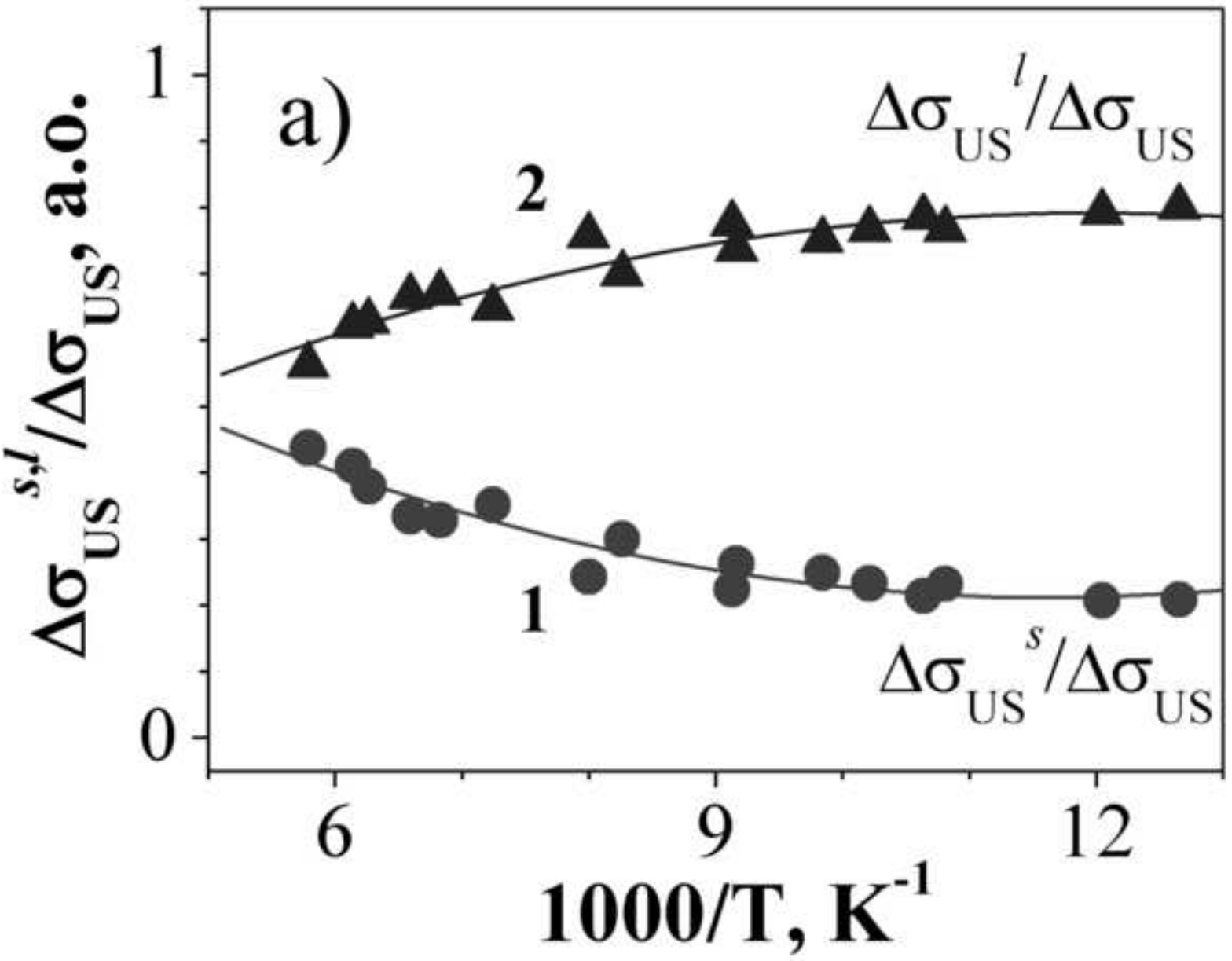

Figure

Click here to download Figure Fig. 4b.jpg

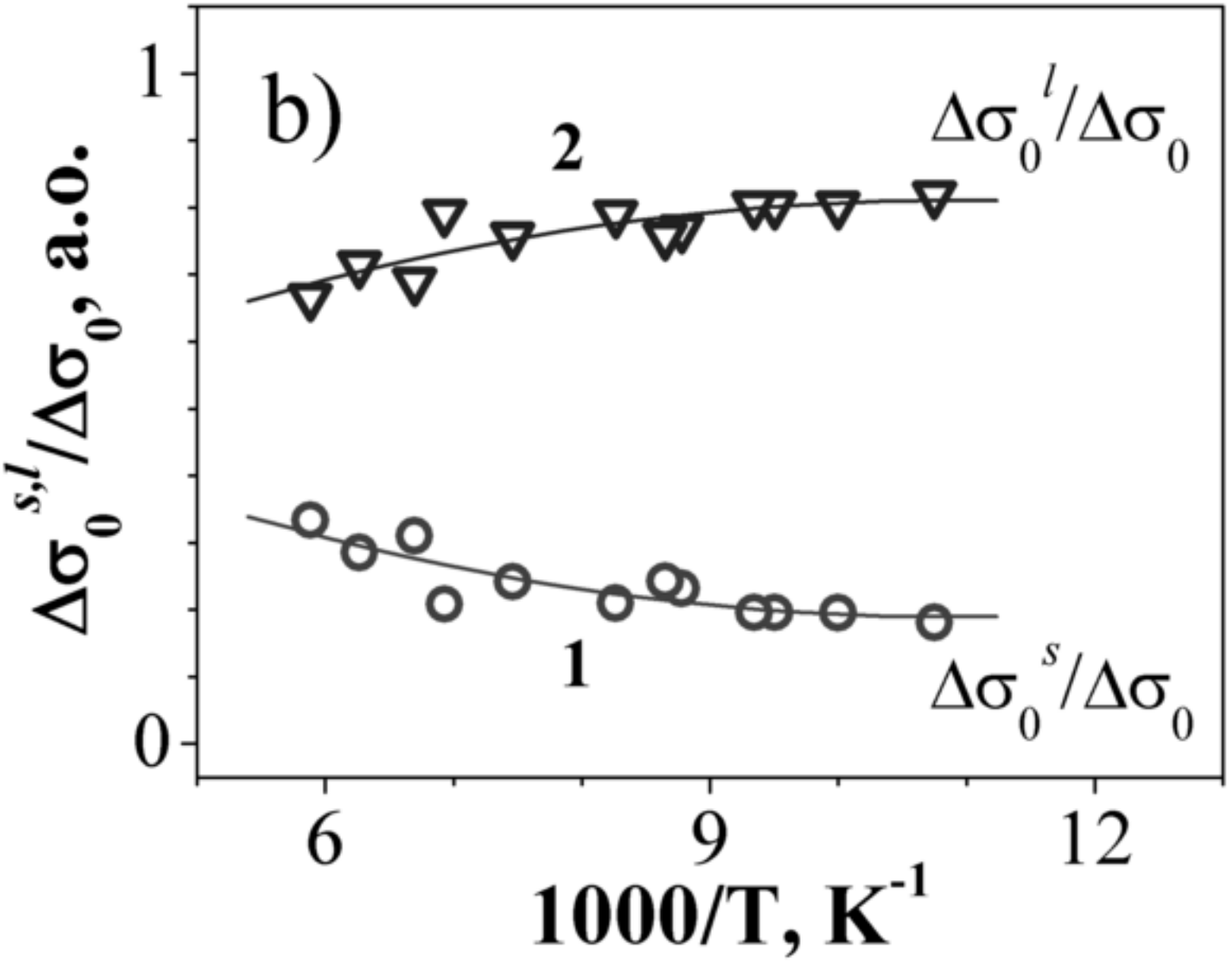

Figure

Click here to download Figure Fig. 5.jpg

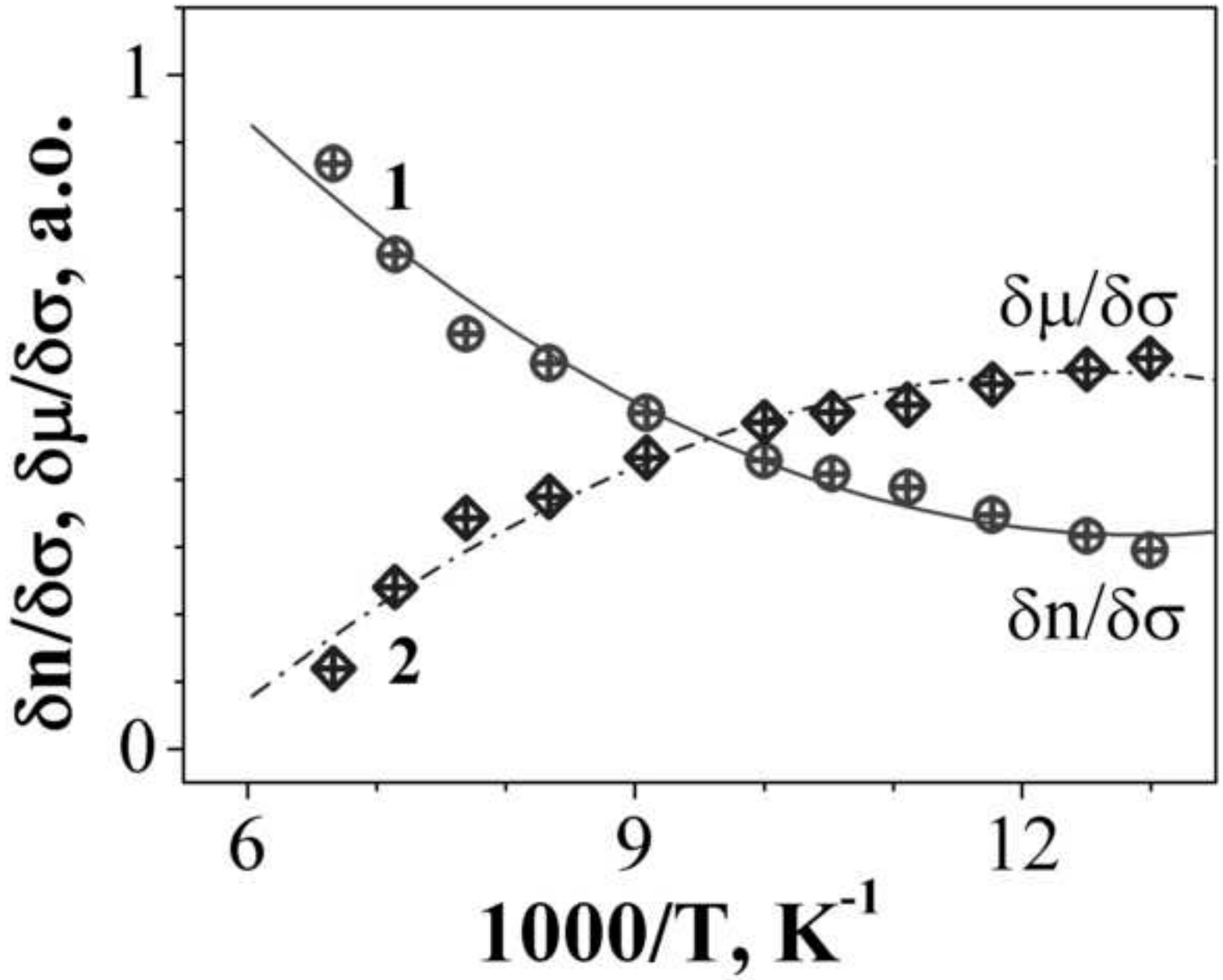

Figure

Click here to download Figure Fig. 6.jpg